Originally published as:

Schmitz, C., Lotze-Campen, H., Gerten, D., Dietrich, J. P., Bodirsky, B., Biewald, A., Popp, A. (2013): Blue water scarcity and the economic impacts of future agricultural trade and demand. - Water Resources Research, 49, 6, 3601-3617

DOI: 10.1002/wrcr.20188

WATER RESOURCES RESEARCH, VOL. 49, 3601–3617, doi:10.1002/wrcr.20188, 2013

Blue water scarcity and the economic impacts of future agricultural trade and demand

Christoph Schmitz,[1,2] Hermann Lotze-Campen,[1] Dieter Gerten,[3] Jan Philipp Dietrich,[4] Benjamin Bodirsky,[1,5] Anne Biewald,[1] and Alexander Popp[4]

Received 6 August 2012; revised 4 February 2013; accepted 8 March 2013; published 21 June 2013.

[1] An increasing demand for agricultural goods affects the pressure on global water resources over the coming decades. In order to quantify these effects, we have developed a new agroeconomic water scarcity indicator, considering explicitly economic processes in the agricultural system. The indicator is based on the water shadow price generated by an economic land use model linked to a global vegetation-hydrology model. Irrigation efficiency is implemented as a dynamic input depending on the level of economic development. We are able to simulate the heterogeneous distribution of water supply and agricultural water demand for irrigation through the spatially explicit representation of agricultural production. This allows in identifying regional hot spots of blue water scarcity and explicit shadow prices for water. We generate scenarios based on moderate policies regarding future trade liberalization and the control of livestock-based consumption, dependent on different population and gross domestic product (GDP) projections. Results indicate increased water scarcity in the future, especially in South Asia, the Middle East, and north Africa. In general, water shadow prices decrease with increasing liberalization, foremost in South Asia, Southeast Asia, and the Middle East. Policies to reduce livestock consumption in developed countries not only lower the domestic pressure on water but also alleviate water scarcity to a large extent in developing countries. It is shown that one of the two policy options would be insufficient for most regions to retain water scarcity in 2045 on levels comparable to 2005.

Citation: Schmitz, C., H. Lotze-Campen, D. Gerten, J. P. Dietrich, B. Bodirsky, A. Biewald, and A. Popp (2013), Blue water scarcity and the economic impacts of future agricultural trade and demand, *Water Resour. Res.*, *49*, 3601–3617, doi:10.1002/wrcr.20188.

1. Introduction

[2] More than ever before, the question of water scarcity shapes debates on current and future food production [*Rosegrant et al.*, 2009; *Hanjra and Qureshi*, 2010; *Godfray et al.*, 2010]. Water scarcity is mainly driven by population growth [*Falkenmark et al.*, 1989; *Vörösmarty et al.*, 2000] and is, from this perspective, a relatively new phenomenon in human history [*Kummu et al.*, 2010]. As global population is expected to grow to 9–10 billion by the middle of the 21st century [*Lutz et al.*, 2001], water scarcity is expected to increase. Furthermore, disposable incomes in developing countries will continue to rise [*Rosegrant and Cline*, 2003] and recent changes in diets of industrial countries will likely be adopted by many developing societies in the near future [*Pingali*, 2006]. This will lead to higher consumption of livestock products [*Delgado*, 2003] and aggravate stress on water resources, as animal-based calories are produced in a much more water-intensive way than plant-based calories [*Hoekstra and Chapagain*, 2007].

[3] The focus of this study is on blue water located in surface water and aquifers, which is defined as the rainfall water escaping evaporation [*Falkenmark et al.*, 2007]. Several indicators have been evolved to measure blue water scarcity. Calculations of water scarcity started with the Falkenmark indicator, relating total freshwater resources to per capita requirements [*Falkenmark*, 1989]. In contrast to the absolute Falkenmark indicator, several relative indicators compute the water withdrawal-to-availability (WTA) ratio [*Vörösmarty et al.*, 2000; *Alcamo et al.*, 2003; *Oki and Kanae*, 2006; *Islam et al.*, 2006; *Hanasaki et al.*, 2008b]. *Smakhtin et al.* [2004] went a step further by adding environmental aspects to the WTA analysis. Another group of indicators emphasizes the social dimension of water scarcity. *Ohlsson* [2000] uses an indicator based on an aggregation of

Additional supporting information may be found in the online version of this article.

[1]Climate Impacts and Vulnerabilities (RD2), Potsdam Institute for Climate Impact Research (PIK), Potsdam, Germany.
[2]Department of Agricultural Economics and Social Sciences, Humboldt University, Berlin, Germany.
[3]Earth System Analysis (RD1), Potsdam Institute for Climate Impact Research (PIK), Potsdam, Germany.
[4]Sustainable Solutions (RD3), Potsdam Institute for Climate Impact Research (PIK), Potsdam, Germany.
[5]Economics of Climate Change, Technical University Berlin, Berlin, Germany.

Corresponding author: C. Schmitz, Climate Impacts and Vulnerabilities (RD2), Potsdam Institute for Climate Impact Research (PIK), D-14473 Potsdam, Germany. (schmitz@pik-potsdam.de)

0043-1397/13/10.1002/wrcr.20188

established hydrological indices and the U.N. human development index (HDI) as an approximation for the social adaptive capacity of a society. More comprehensiveness is provided by the watershed sustainability index [*Chavez and Alipaz*, 2007], where in addition to HDI, the water poverty index and the environmental sustainability index (ESI) are considered. A first attempt of a rather simple economic water scarcity indicator has been designed by the International Water Management Institute [*Molden*, 2007]. A region is called economic water scarce, if a lack of investment in water infrastructure or a lack of human capacity to satisfy the demand for water is observed.

[4] In our study, we look explicitly on agricultural fresh water use, since around 70%–80% of human freshwater withdrawals [*Gleick et al*., 2009] and around 90% of the consumed blue water [*Shiklomanov and Rodda*, 2003] are used for agriculture. A specific indicator for agricultural water stress has been recently developed by *Vörösmarty et al*. [2010]. The authors have estimated the burden that crop production places on renewable water resources by considering water supply and irrigation water demand. *Gerten et al*. [2011] follows a similar approach but calculates the WTA ratio based on blue and green water availability; with green water defined as water originating directly from precipitation.

[5] Although all of those indicators have different perspectives on water scarcity, they consistently lack crucial economic processes. None of the indicators has an integrated view based on the interplay between biophysical availability of water and economic-driven demand [*Sauer et al*., 2010]. As *de Fraiture* [2007] points out, current indicators solely focus on the water and biophysical sector and largely ignore macroeconomic drivers, such as income, trade, and economic policy as well as microeconomic drivers, such as production costs and productivity growth. To fill large parts of this gap, we have developed a new agroeconomic water scarcity indicator on grid cell level, which considers blue water used for irrigation agriculture. The indicator is based on the water shadow price (WSP) generated uniquely through the coupling of a global biophysical vegetation model and an economic land use model. The indicator has the advantage of including economic processes and drivers, such as production costs, technological change (TC), and international trade. This allows for analyzing policies in an international context by taking economic processes related to land use endogenously into account. The IMPACT-WATER model [*Cai and Rosegrant*, 2002], the related WATERSIM model [*de Fraiture*, 2007], and the Global Trade Analysis Project - Water (GTAP-W) model [*Calzadilla et al*., 2011b] are approaches to integrate the economics of water into an agricultural modeling framework. Although the first two models are partial equilibrium models, focusing on the agricultural sector, GTAP-W is a computable equilibrium model (CGE) taking all economic sectors into account. These models are well suited for the short- and medium term and have the strength to be very detailed on economic parameters. However, in contrast to our approach, they are neither working on a high spatial resolution nor are they directly linked to a biophysical model. Both features are essential for analyzing local phenomena, such as water scarcity.

[6] In our analysis, we focus on two possible policy areas and their interaction. The first is the option of increased food trade via trade liberalization. Agricultural goods contain a significant amount of so-called virtual water, which is defined as the amount of freshwater embedded in the production process [*Hoekstra and Chapagain*, 2007)]. Trading goods internationally plays an important role for increasing the global efficiency of water use [*Fader et al*., 2011]. Several studies have quantified the importance of current virtual water trade and demonstrated that some water-scarce regions are major importers of water-intensive products [*Konar et al*., 2011; *Fader et al*., 2011; *Hanasaki et al*., 2010; *Chapagain and Hoekstra*, 2008; *Hoekstra and Hung*, 2005; *Oki and Kanae*, 2004]. In contrast to virtual water assessments, we explicitly analyze the effects of different trade liberalization scenarios on agroeconomic water scarcity and assess the impact on future water scarcity.

[7] The second policy parameter enforces a changing diet toward lower consumption of animal products. At the turn of the millennium, around 2 billion people based their diets largely on animal products, whereas more than 4 billion people lived primarily on a plant-based diet [*Pimentel and Pimentel*, 2003]. No global study has assessed the impact of changing diets on global water resources in detail. *Gerten et al*. [2011] has assessed the sensitivity of their results by calculating the likelihood of water scarcity under a scenario of lower animal calorie intake. *Renault and Wallender* [2000] have analyzed in a simple regional model the percentage of additional water that could be saved according to different scenarios until 2025. Apart from those studies, the influence of changing diets has been either shown globally on land use [*Wirsenius et al*., 2010] and greenhouse gas emissions [*Popp et al*., 2010; *Stehfest et al*., 2009] or regionally on water consumption [*Liu and Savenije*, 2008]. Finally, in order to evaluate the sensitivity of the simulations, we run the model with different population and gross domestic product (GDP) scenarios.

[8] We start our analysis by describing the involved models, the creation of the agroeconomic water scarcity indicator, and the scenario implementation. Furthermore, water-related input data, i.e., water discharge and irrigation demand from the dynamic global vegetation and water balance model Lund-Potsdam-Jena managed Land (LPJmL) [*Bondeau et al*., 2007], are compared with the outcome of the global water resources model H08 [*Hanasaki et al*., 2008a, 2008b]. In section 3, we present the outcome of the scenarios with a special attention to WSPs, TC rates, and land use changes as well as the sensitivity of the results. Subsequently, we discuss methods and results in relation to previous studies. In the last section, we draw conclusions and policy implications from our analysis.

2. Modeling Approach and Methods

2.1. Model Descriptions

2.1.1. MAgPIE Model

[9] For the analysis, we use model of agricultural production and its impact on the environment (MAgPIE), a nonlinear recursive dynamic optimization model [*Lotze-Campen et al*., 2008; *Schmitz et al*., 2012]. It is linked to the dynamic vegetation model LPJmL on a 0.5° resolution (see section 2.1.2), to simulate spatially explicit land and water use patterns. This approach provides a high flexibility to integrate various types of biophysical constraints into an

economic decision-making process. The dual solution of the economic optimization model MAgPIE allows for computing shadow prices (or implicit economic values) for binding constraints on grid cell basis. The shadow prices define the potential cost savings the model would achieve by relaxing the constraint by one unit. In this study, we focus on the WSP, which reflects the implicit economic value for one additional cubic meter of water in a particular grid cell (see section 2.2.3).

[10] Each grid cell is assigned to 1 of the 10 economic world regions (Appendix A, Table A1). The initialization year is 1995 with data on income (GDP) [*World Bank*, 2001], population [*Center for International Earth Science Information Network (CIESIN)*, 2000], demand for food energy [*Food and Agriculture Organization (FAO)*, 2010], average costs for different production activities [*Narayanan and Walmsley*, 2008], and food self-sufficiency ratios [*FAO*, 2010]. All activities on the supply side are specific for each grid cell (0.5° resolution), whereas activities on the demand side are aggregated to the regional level. Future demand of calories and the share of livestock products are dependent on income and population, and they are based on a detailed regression analysis (Figure 1 and Appendix B).

[11] With flexible minimum self-sufficiency ratios, MAgPIE is able to represent international trade and allocates global food demand to the supply regions. Agricultural self-sufficiency ratios describe the ability of countries to produce as much food as they demand. As an example, a country with a self-sufficiency of 0.75 for wheat produces 75% of its demand by itself and imports 25%. In MAgPIE, two virtual trading pools are implemented, which distribute the demand to the 10 regions in a different way (Figure 1). The fixed trade pool (first pool) allocates the demand according to self-sufficiency ratios based on Food and Agriculture Organization (FAO) food balance sheets [*FAO*, 2010]. The self-sufficiency ratios assign the quantity that is produced domestically, and the corresponding export shares [*FAO*, 2010] define the share of the regions in global exports. The free trade pool (second pool) distributes the demand to the supply regions according to comparative advantage criteria. This means that the region with the lowest production costs per ton will export. The parameter p^{tb} determines the share of demand for each of the two pools. If p^{tb} equals 1, total demand will be allocated according to the predefined self-sufficiency ratios and the export shares to the supply regions. If p^{tb} is equal to 0, all trading quantity will hit the second pool and is allocated according to comparative advantages. More details of the implementation are provided in *Schmitz et al*. [2012] and in the mathematical description in Appendix C.

[12] The resulting demand calories are produced by 16 cropping activities and 5 livestock activities (see Appendix A). The five livestock activities depend on specific feed energy requirements derived from *Wirsenius* [2000], which consist of a mixture of pasture, fodder, and food crops. All these inputs are specific for each region and animal type and are on the basis of preconditions for lactation, maintenance, reproduction, growth, and various other biological needs. Inputs for the calculation of feedstock (crops, byproducts, and pasture) and livestock-related greenhouse gas emissions in MAgPIE are calculated in *Weindl et al*. [2010].

[13] For future projections, the model works on time steps of 10 years in a recursive dynamic mode. The land use pattern of each period is used as the initial land pool for the consecutive period. MAgPIE minimizes global costs, consisting of four different cost categories: First, production costs, containing factor costs for labor, capital, and intermediate inputs, are taken from GTAP [*Narayanan and Walmsley*, 2008]. Production costs per area unit evolve with the yield level in a linear relationship [*Schmitz et al*., 2010]. Second, investments in yield-increasing TC increase exponentially based on the state of agricultural development of a region [*Dietrich* et al., 2012; *Dietrich* et al. 2013]. This endogenous implementation allows MAgPIE to project future yield increases and the costs involved. In terms of water, TC increases demand for blue water, since water requirements are dependent on yield. Third, costs for land expansion which is the other alternative for MAgPIE to increase food production [*Krause et al*., 2009; *Popp et al*., 2011] and costs for irrigation area expansion are considered. Land conversion costs (for the conversion of forest into cropland) are based on marginal access costs on country level from the global timber model [*Sohngen et al*., 2009]. Additionally, expansion of irrigation area involves regional costs, which were aggregated from the AQUA-STAT-Database [*FAO*, 2011]. Fourth, intraregional transport costs accrue for every commodity unit as a function of the distance to intraregional markets, the quality of the infrastructure (both based on a detailed data set on travel time [*Nelson*, 2008]) and average transport costs (based on GTAP [*Narayanan and Walmsley*, 2008]). A mathematical description of the model is provided in the supporting information.

2.1.2. LPJmL Model

[14] Biophysical inputs for MAgPIE, such as potential crop productivity and related water use as well as land and water constraints, are supplied for each grid cell (0.5° resolution) by the Lund-Potsdam-Jena dynamic global vegetation and water balance model with managed Land (LPJmL) [*Bondeau et al*., 2007]. LPJmL models dynamic processes linking biophysical processes like soil and climate conditions, plant growth and water availability, and directly considers the impacts of CO_2, temperature and radiation on agricultural yields. For this study, however, those inputs are not subject to any climate change impacts. LPJmL also covers surface and subsurface water flows (though without explicit distinction of groundwater), as carbon and water-related processes are closely linked in plant physiology. Also, blue and green water consumption is separated, with the former occurring on areas equipped for irrigation [*Döll and Siebert*, 2000], which allows for the distinction of rainfed and irrigated yields. Green water originates directly from precipitation and is taken up by plants and soil. Blue water is the amount of evapotranspiring irrigation water originating from rivers, lakes, aquifers, and reservoirs [*Gerten et al*., 2004]. The computation of blue water stocks and flows and the separation of blue and green water flows on irrigated areas in LPJmL are illustrated in detail in *Rost et al*. [2008]. The river-routing module in LPJmL distributes the natural runoff and its downstream movement as additional water to irrigated areas (see *Rost et al*. [2008] for a detailed description of this module). The water discharge value for each grid cell from LPJmL is used as a

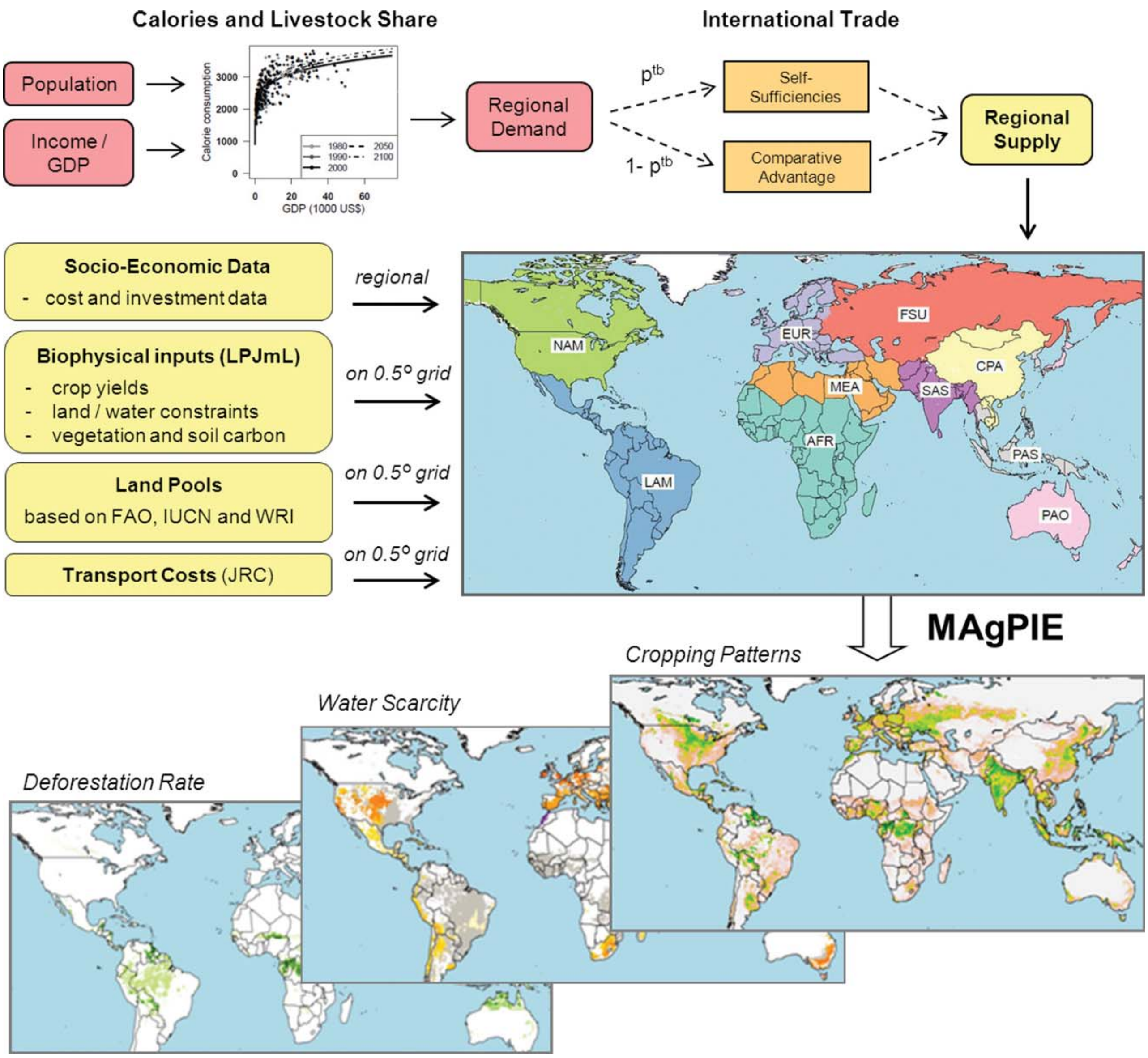

Figure 1. Simplified MAgPIE flowchart of key processes highlighted in this study (demand and trade implementation, data inputs from LPJmL and spatially explicit WSP). With exogenous data about population and GDP development, we calculate regional demand and the livestock share. The former is then translated to regional supply depending on the international trade scenario. Further inputs for MAgPIE are socioeconomic data like production costs and biophysical inputs from LPJmL. After the optimization of MAgPIE, one of the outputs is cropping patterns of the different crops, which is the basis for the WSP.

constraint for irrigation in MAgPIE. From a modified version of the MIRCA2000 land use data set [*Portmann et al*., 2010], the information about rainfed and irrigated land use fractions is derived [*Fader et al*., 2010].

2.2. Blue Water Implementation and Related Shadow Price

[15] The implementation of blue water in MAgPIE is based on data inputs from LPJmL. LPJmL delivers two relevant cell-specific water inputs for MAgPIE: First, blue water discharge available to the agricultural sector, and second, the water requirement per plant and cell that is needed for irrigation. For this analysis, we compared those inputs with the outcome of an independent hydrology model (section 2.2.1). The water discharge from LPJmL is reduced in MAgPIE by an efficiency factor that represents the losses in the water and irrigation system (section 2.2.2). Finally, the WSP can be determined based on the water consumption per cell calculated in MAgPIE (section 2.2.3).

2.2.1. Comparison of Water Inputs

[16] Both LPJmL inputs blue water discharge and water requirement per plant are crucial factors for the analysis. Therefore, for an evaluation use analogous results from the H08 model, which similar to LPJmL provides water-withdrawal values specifically for agriculture on a grid cell level (*Hanasaki et al*. [2008a] and applied in *Hanasaki et al*. [2008b]). For comparison, we computed the WTA ratio from both models, where the model runs are based on

climate projections from the general circulation model European Centre Hamburg Model 5 (ECHAM5) [*Roeckner et al.*, 2003] and special report on emission scenarios (SRES A2) [*Nakicenovic and Swart*, 2000]. We followed the approach by *Vörösmarty et al*. [2010] and ranked it relatively to the highest value. This means the highest value is equal to 1, whereas the lowest value is almost 0. In total, 14,382 cells of 59,199 cells contain a WTA ratio in both models. With the help of the map comparison kit [*Visser and de Nijs*, 2006], which allows for the numerical comparison of two different maps, we compared both maps. The comparison index c is calculated by taking the difference of both model indices on cell level j.

$$c_j = \text{H08}_j - \text{LPJmL}_j. \tag{1}$$

[17] Figure 2a illustrates the ranked agricultural WTA ratio calculated for the LPJmL model and the graph in the middle for the H08 model. Highest values are modeled for southeast Australia, northern China, north India, Pakistan, the Middle East, north Africa, southern Europe, and parts of the United States and Mexico. The map in the middle shows the same for H08 model (Figure 2b).

[18] Figure 2c shows the difference of the ranked WTA ratio between the H08 model and the LPJmL model. Largest differences are in Southern Europe and Turkey, where LPJmL has higher WTA values and for southern China, where LPJmL has lower values than H08. The validation discloses that both data sets, although independently derived (LPJmL is primarily a vegetation model, while H08 is a specialized hydrology model), the outcomes are very similar. Comparing the LPJmL outputs with the recently published indicator by *Vörösmarty et al*. [2010], it appears that the LPJmL values are higher in Western United States and Middle East and lower in Central Asia and Argentina, whereas the remaining regions are similar.

2.2.2. Irrigation Efficiency

[19] Improving irrigation efficiency is one of the main options to reduce water consumption [*Molden*, 2007]. More than 50% of global water resources, which are intended for irrigation, are lost due to bad management, losses in the conveyance system, and inefficient application to the plant [*Rogers et al*., 1997]. In MAgPIE, irrigation efficiency is implemented through an efficiency factor that comprises management, conveyance, and application efficiency. The data are from *Rohwer et al*. [2007], who calculated specific efficiency levels for 134 countries for the year 1995. In contrast to most other studies, irrigation efficiency in MAgPIE is a dynamic input. In order to project future irrigation efficiencies, we tested several hypotheses concerning the relationship between the efficiency factor and independent variables, such as GDP per capita [*Heston et al*., 2011], irrigation area share [*Döll and Siebert*, 2000], and the level of agricultural intensity [*Dietrich* et al., 2012]. Cross-sectional regression analyses with different functional forms reveals that only GDP per capita is significant as an explanatory variable for irrigation efficiency. For the analysis, we included 149 countries with documented irrigation areas. However, in order to reduce data errors by small countries (with respect to irrigated agriculture), those below an irrigation area share 5% of total cropland, and an absolute irrigation area of 3 million hectare was

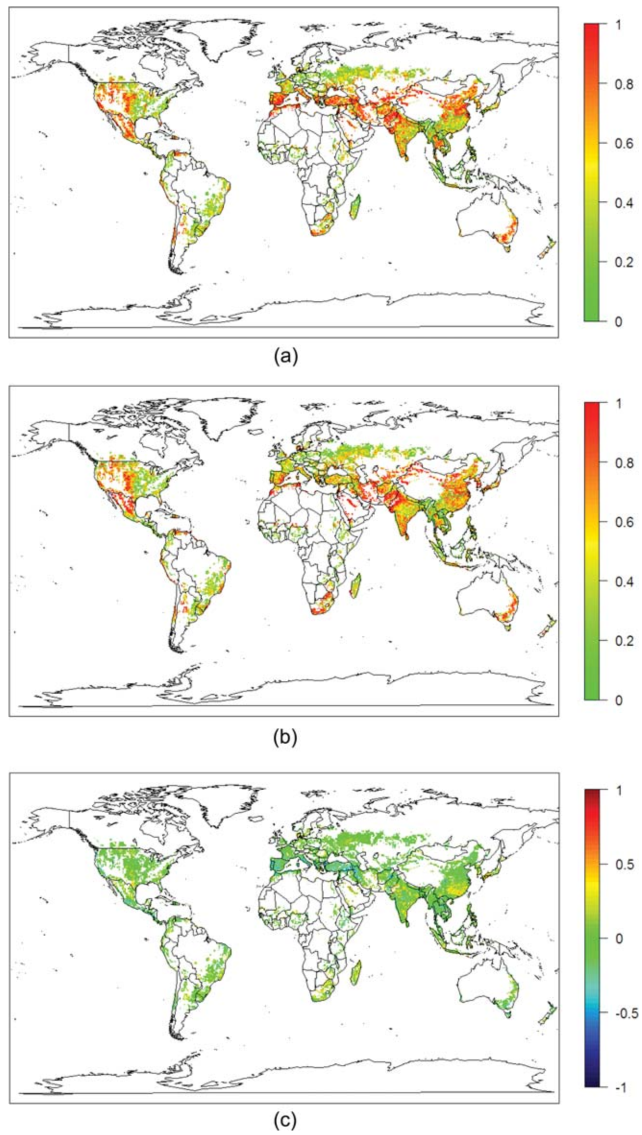

Figure 2. Upper and central map: (a) Relative ranked ratio of water WTA of the LPJmL model and the (b) H08 model in 1995. Values of both graphs are displayed as share compared to the highest rank with 1 as the highest value and 0 the lowest. Lower map: (c) Comparison between ranked WTA ratio of LPJmL and H08 model.

clustered together to nine world regions. Together with the 13 countries, which fulfilled the minimum criteria, 22 data points have been used for the regression.

[20] The regression determines the following linear relationship between the level of economic development (measured in GDP per capita $\text{gdp}_i/\text{pop}_i$) and irrigation efficiency η on regional level i:

$$\eta_i = 0.381 + \left(\frac{\text{gdp}_i}{\text{pop}_i}\right) 5.28 \times 10^{-6}. \tag{2}$$

[21] The results of the weighted linear regression gave an adjusted R^2 of 0.55, but highly significant P-values of the t-tests for the constant and the slope ($P = 0.000$). The conducted regression specification error test (RESET)

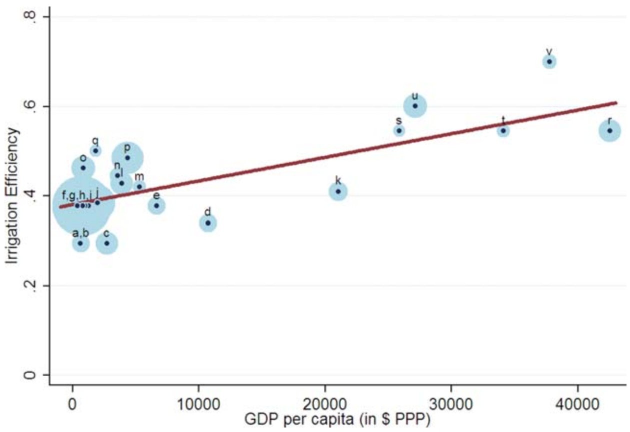

Figure 3. Regression between irrigation efficiency and GDP per capita (in \$PPP/capita). a = Vietnam, b = Pakistan, c = Thailand, d = Central America, e = Turkey, f = Bangladesh, g = Indonesia, h = India, i = Philippines, j = Central Asia (including China), k = rest of South Asia, l = rest of former Soviet Union, m = Malaysia, n = Middle East/north Africa, o = Sub-Saharan Africa, p = South America, q = Ukraine, s = Spain, r = North America, t = France, u = rest of Europe, v = Pacific OECD Countries

[*Ramsey*, 1969] offers a high significance level, which means that no important variables seem to be omitted ($F[3, 18] = 1.59$ and $F_{0.05} = 3.16$). Figure 3 shows the graph of the regression analysis with the corresponding countries and regions.

[22] The irrigation efficiencies increase over time due to increasing GDP per capita in all regions (Figure D1 in Appendix D). Highest efficiencies are achieved in developed regions, like North America (NAM) (from 56% in 2005 to 67% in 2045) and Europe (EUR) (from 48% to 60%), and Pacific OECD (PAO) (from 51% to 62%). Europe is behind NAM, since the Eastern European countries have very low values. Sub-Saharan Africa (40%) and South Asia (42%) have the lowest efficiencies in 2045.

[23] Finally, in MAgPIE available water for irrigation, p^{water} is calculated on cell level j by the product of water discharge $p^{discharge}$ and the regional specific irrigation efficiency η_i.

$$p_j^{water} \le p_j^{discharge} \cdot \eta_i. \quad (3)$$

2.2.3. Water Shadow Price

[24] Since MAgPIE is an economic optimization model operating under constrained conditions, it is possible to generate a shadow price for every independent constraint. The shadow price is defined as an achievable rate of increase in the objective function per unit increase in resource x [*Aucamp and Steinberg*, 1982]. Because our objective function minimizes costs, we have to reframe the definition to "the achievable rate of decrease in the objective function if the constraint x is relaxed by one unit." For our analysis we, use the available water constraint p_j^{water}.

$$\text{wsp}_j = \frac{\partial g_t^*}{\partial p_j^{water}}, \quad (4)$$

where wsp_j stands for the water shadow price in each cell j and g_t^* denotes the optimal value of the goal function (defined in the supporting information). The water constraint for each cell j is defined as

$$\sum_v x^{area}_{t,j,v,'ir'} p^{yield_{t,c}}_{t,j,v,'ir'} p^{watreq}_{j,v} + \sum_l x^{prod}_{t,j,l} \, p^{watreq}_{j,l} \le p_j^{water}, \quad (5)$$

where $x^{area}_{t,j,v,'ir'}$ is the total irrigated area of each crop v, each cell j, and each time step t; $p^{yield_{t,c}}_{t,j,v,'ir'}$ is the irrigated yield (including TC) for each time step, each cell, and each crop; $p^{watreq}_{j,k}$ is the cellular water requirements for product (v for crops and l for livestock); $x^{prod}_{t,j,l}$ is the total production of each livestock product l, for each cell at each time step. From the constraint specification, it follows that the required amount of water is proportional to the production volume. The cellular water available for production sets the limit for the consumption for water in each cell.

[25] In economic terms, wsp is defined as the saved marginal costs, when one additional unit of water would be available in a particular grid cell. With cell-specific WSPs we are able to generate maps in order to define hot spots of water scarcity under different future scenarios.

2.3. Scenario Definition and Sensitivity Analysis

[26] We consider one reference scenario and three policy scenarios which are based on medium population and GDP projections. The reference scenario is based on the description in section 2.1.1. It is assumed that 50% of the intact and frontier forest (which is mainly the rainforest in South America, central Africa, and Pacific Asia) must be saved until 2045. Furthermore, we do not model different climate change scenarios in this study. The three policy scenarios differ from the reference scenario in their policies regarding trade liberalization and the consumption of livestock products (Table 1). We created those scenarios with the aim to consider a range of future policies, and, therefore, we chose moderate scenarios. This contrasts with many other studies, which usually present extreme scenarios in order to characterize the theoretical range.

[27] We assume two different trade policies [cf. *Schmitz et al.*, 2012]. The bilateral trade implementation reflects the case that no new global trade agreement is implemented. It reflects largely the situation under the Doha World Trade Organization (WTO) Negotiation Round of the past decade, during which a joint trade agreement could not be agreed upon. In contrast, our global trade policy scenario follows a historically derived pathway of trade liberalization, considering the two decades before the Doha Round (1980–2000). The trade study by *Dollar and Kraay* [2004] found out that between the 1980s and 1990s nonglobalizing countries have cut tariffs by 22%, globalizing countries by 11%, and rich countries by 0%. Hence, as a plausible

Table 1. Scenario Definition

Scenarios	Demand Pattern	
Trade liberalization	BAU Diet	Healthy livestock diet
Bilateral	Reference (0)	Livestock (2)
Global	Trade (1)	Trade-livestock (3)

Table 2. Trade Barrier Reduction Factor in the Two Trade Scenarios Over Time

Scenario	2005	2015	2025	2035	2045
Bilateral trade liberalization	1	0.975	0.951	0.927	0.904
Global trade liberalization	1	0.9	0.81	0.729	0.656

policy scenario, we chose a 10% trade barrier reduction in each decade until 2045. This is supported by various other literature sources [*Healy et al.*, 1998; *Conforti and Salvatici*, 2004], which assume that global trade agreements are successful in the future. Table 2 displays the development of the trade balance parameter over time in the different trade implementations.

[28] In the business-as-usual diet scenario (BAU diet), the continuation of current trends in animal consumption is assumed and the share of consumed livestock products depends on the GDP per capita scenarios (see Appendix B). In the second scenario, all regions continuously develop their dietary habits toward an average livestock calorie consumption of 20% per capita until 2045. The 20% share of livestock-based calories is taken as a policy threshold, since it is considered as a nutritionally balanced and healthy diet for society [*Pimentel and Pimentel*, 2003]. Although there is a lively scientific debate around this topic and other studies suggest that a pure vegetal-based diet would be even the healthiest [*Campbell and Campbell*, 2006], we take the 20% share as a policy target, which might be realistic to achieve in 2045. Figure B2 in Appendix B shows the animal-based calorie share for the period 2005–2045 in both scenarios.

[29] Both policy scenarios, trade liberalization and the reduction of animal-based calories, are applied to the 10 regions in MAgPIE. Although this regional aggregation is quite broad, the countries within the regions are quite homogenous in terms of trade policy and the consumption of animal products. An exception is the region PAO comprising Australia, New Zealand, and Japan, which differ considerable in terms of trade policy and the composition of diets. The outcome of the model depend to a large extent on the food demand requirements, which in turn depend on the respective population scenarios and on a regression with GDP per capita (see Appendix B). In order to reveal the sensitivity and variation in the results, we apply a combination of three different U.N. population [*United Nations (UN)*, 2011] and three different GDP scenarios which result in nine different scenarios for food demand (Table B1). From these, we take one (scenario E) as default scenario for the analysis and the remaining eight as sensitivity scenarios. For the methodology, we refer to Appendix B.

3. Scenario Results

3.1. Water Shadow Price

[30] The cell-specific WSP of MAgPIE is plotted for the years 2005 (Figure 4a) and 2045 (Figure 4b) on a 0.5 grid basis. We note three regions, South Asia (India, Bangladesh, Pakistan, and Afghanistan), north Africa (Morocco, Algeria, and Egypt), and the Middle East (with Israel, Saudi Arabia, and Iran), where the WSP is expected to reach much higher levels in the future. Foremost, blue water scarcity in countries such as Morocco, Israel, and Iran increases from around 0.7 US\$/m^3 in 2005 to up to 2 US\$/m^3 in 2045. Almost the whole area of South Asia is predicted to face an increase in water scarcity within the coming decades given the fact that the WSP is growing to values of 0.6 US\$/m^3 or even higher. Significant higher levels can also be expected in southeastern Australia, northeast and southeast China, Japan, and Europe. In Europe, the highest WSPs are supposed to appear in countries such as France or Germany, and also in Southern Europe, water scarcity is supposed to worsen. The southeast of Australia and Japan as well as the eastern part of China are expected to experience an explicit increase in WSP up to 0.3–0.4 US\$/m^3. On the other hand, the results in some regions, like large parts of South America or the southeast of Africa, indicate that enough freshwater would be available for irrigation in the future, resulting in a WSP equal to zero.

[31] Figure 5 presents the differences in cell-specific WSPs in the three policy scenarios (1–3) compared to the reference scenario (0) in the year 2045 (lower graph in Figure 5). Starting with the trade scenario (1), four regions (South Asia, Middle East/north Africa, southeast Australia, and Japan) reveal striking results. In South Asia and Middle East/north Africa, the WSP is expected to decrease in almost the whole region by up to 0.3 US\$/m^3. In contrast, in southeast Australia and Japan, the price is going to rise by around 0.1 or 0.2 US\$/m^3, respectively. Furthermore, in central Asia (mainly Kazakhstan) and some parts of China, the United States, and southern Africa, small rises are obtained. In Europe, WSPs moderately drop and even less so in large parts of mid and western United States.

[32] In the livestock scenario (2), the WSP decreases in all countries, except for Japan and to a small extent in countries of southern Africa. Highest decreases are obtained particularly in Europe and western United States as well as in southern China. This means that the WSP in Australia and Central Asia increases in the trade scenario (1) and decreases in the livestock scenario (2). However, in the combined trade-livestock scenario (3), southern Africa reveals decreasing WSPs, and only in Japan, prices increase even further. Comparing the third with the second scenario shows that in South Asia with countries like India, Afghanistan, and Bangladesh, the price decrease is highest, followed by southern China, whereas in Europe, the United States, Latin America, north China, and Australia, the differences are only marginal.

[33] In order to stress the differences of the WSP in the different scenarios in 2045 and the sensitivity of those simulations, we aggregated the price on a regional level. The regional WSP in the reference scenario in 2045 (Figure 6) is highest in South Asia (SAS) with a price of almost 0.38 US\$/m^3, followed by Middle East and north Africa (MEA) with almost 0.22 US\$/m^3, EUR with 0.16 US\$/m^3, and centrally planned Asia (CPA) with 0.08 US\$/m^3. All other regions have WSPs below 0.04 US\$/m^3. Considerable low WSPs are projected for sub-Sahara Africa (AFR) and Latin America (LAM) with less than 0.01 US\$/m^3. The boxplots display the variation (minimum, lower quartile, median, upper quartile, and maximum) due to the nine different population and GDP sensitivity scenarios. The variations are rather moderate, given the large variation in the applied sensitivity scenarios, and the order of regions is almost not influenced by them. Largest variations are obtained for the

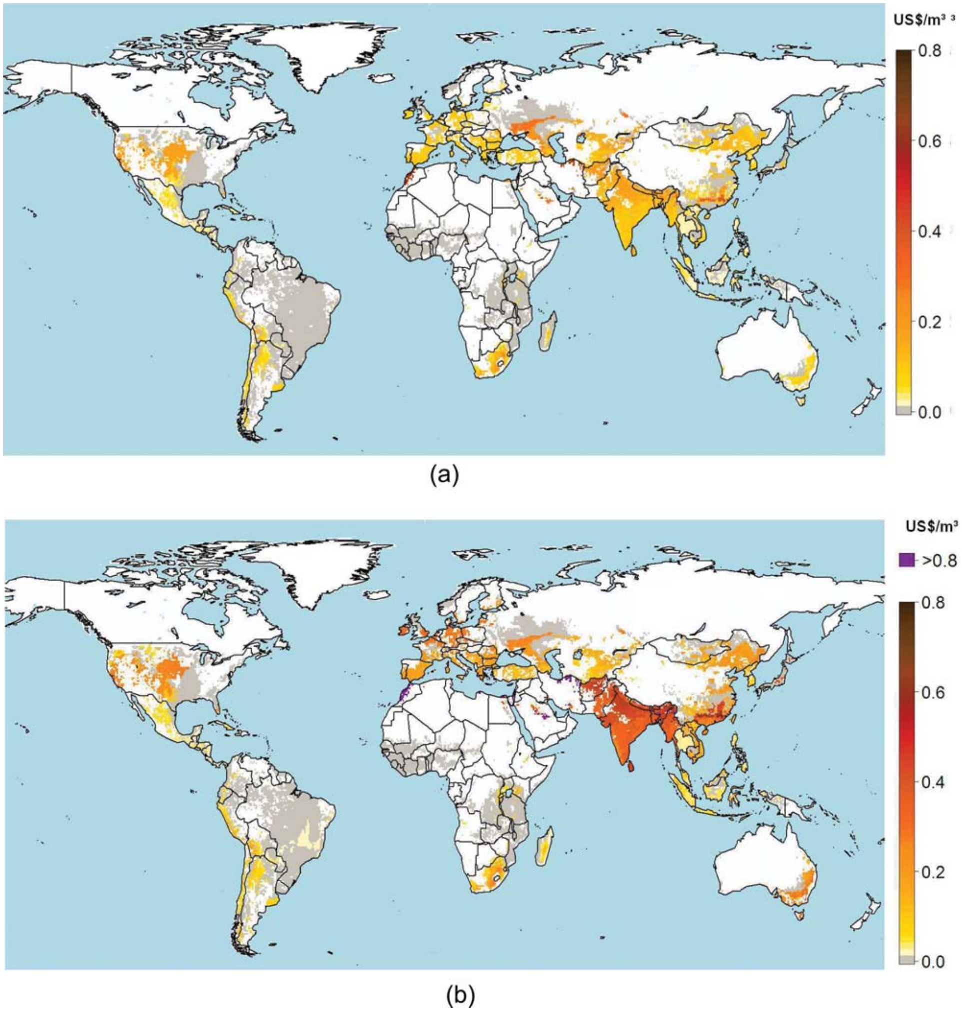

Figure 4. Cell-specific WSP for the reference scenario in (a) 2005 and (b) 2045 on a 0.5 grid basis. White cells do not consist of any cropland equipped for irrigation. Gray cells contain irrigation area but the WSP is zero.

three regions with the highest WSP (EUR, MEA, and SAS). In the case of SAS, the maximum value is 0.53 US\$/m^3 and the lowest value is 0.26 US\$/m^3.

[34] Figure 7 emphasizes the difference in regional WSP in 2045 in the three policy scenarios (1–3) versus the reference scenario (0). Presenting absolute changes in all regions and all scenarios, the shadow price decreases or stays constant. The only exception is the region PAO, where the price increases by 0.02 US\$/m^3 in the trade scenario (1). We obtain again for SAS and MEA the highest decreases. In both regions, the trade scenario (1) shows stronger reductions of the WSP than the livestock scenario (2). The opposite is found for EUR, CPA, PAO, and NAM. In these regions, the combined trade-livestock scenario (3) demonstrates a lower reduction than in the livestock scenario (2) with only bilateral trade liberalization. In contrast, SAS with -0.31 US\$/m^3 and MEA with -0.21 US\$/m^3 have the highest reductions in the combined scenario (3). Pacific Asia (PAS) resembles SAS and MEA as the livestock scenario (2) causes the lowest decrease and the combined scenario the strongest decrease (-0.02 US\$/m^3), but with much lower rates. For former Soviet Union (FSU), we observe only minor changes, and values in AFR and LAM do not change at all. The sensitivity of the results is generally moderate, except for MEA and SAS in the first scenario, for EUR in the second scenario and for all three in the third scenario. The highest reduction is found for SAS in the combined scenario (3) with a value of -0.41 US\$/m^3.

3.2. Technological Change and Land Use Change

[35] Figure 8 displays average annual TC rates for the 10 world regions in the reference scenario. MEA has the highest TC rates over this period with an average annual rate of 1.9%. AFR, CPA, and SAS have high rates as well values more than 1%. EUR and PAO have the lowest values. The rate depends to a considerable extent on the future population and GDP growth as the boxplots show; in some regions less (e.g., LAM and FSU) in some regions more (e.g. MEA, SAS, and PAS).

[36] In Figure 9, we present the differences in the regional TC rates (presented in percentage points (pp)) of the three policy scenarios compared to the reference scenario over the period 2005–2045. The most notable region is MEA showing decreases of up to 1 pp in the two global

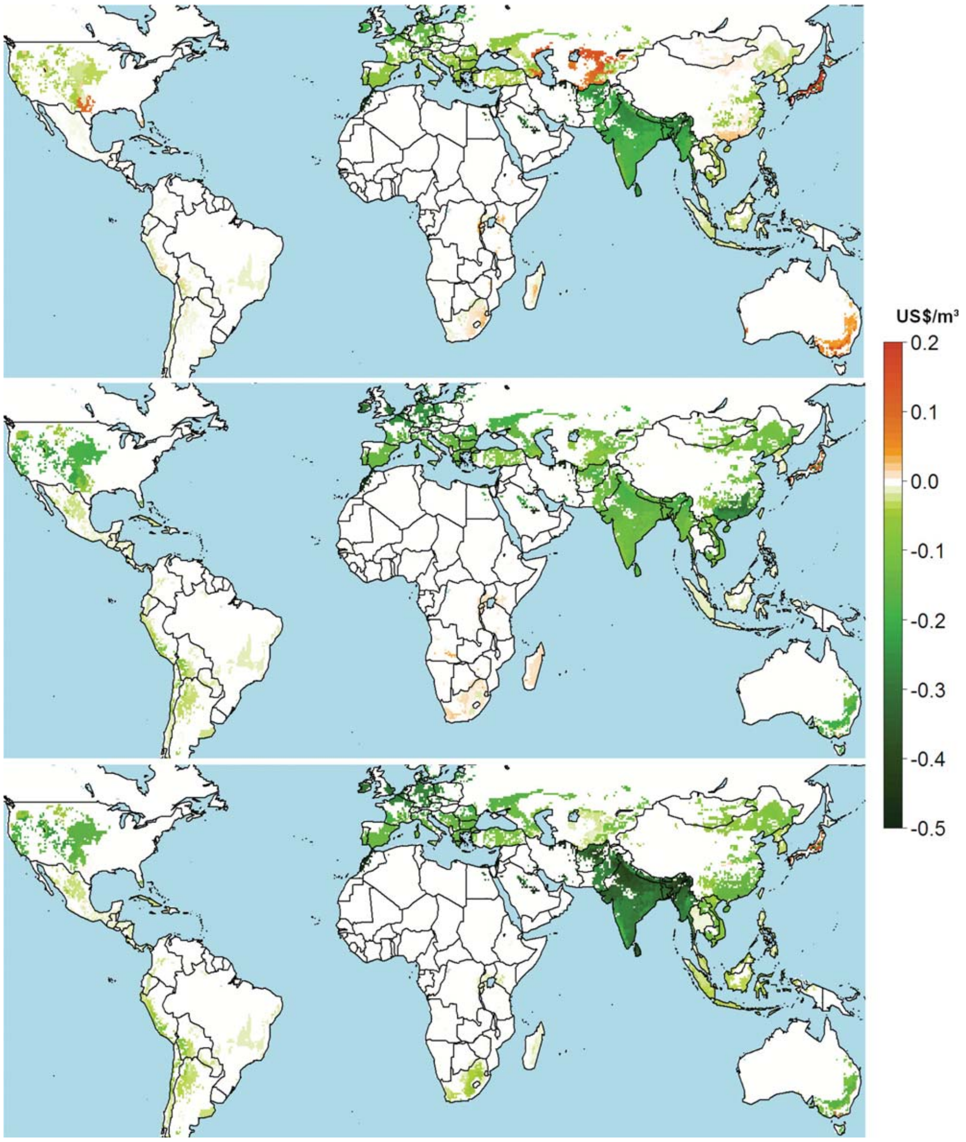

Figure 5. Differences in the cell-specific WSP in the scenarios 1-trade (upper map), 2-livestock (central map), and 3-trade-livestock (lower map) compared to the reference scenario (0) in 2045 on a 0.5 grid basis.

trade liberalization scenarios. In the livestock scenario (2), however, TC rates are reduced by less than 0.5 pp. A similar behavior can be expected in SAS, although the reductions in TC are not as high as in MEA, reaching up to 0.84 pp in the combined trade-livestock scenario (3). In CPA, EUR and NAM TC rates are estimated to decrease stronger in the livestock scenario (2) than in the trade scenario (1). In contrast, FSU faces a similar decline of between 0.32 and 0.35 pp in all three policy scenarios. Two regions, AFR and PAO, show rising TC rates within specific scenarios. In AFR, the healthy livestock consumption implies rising TC rates of almost 0.2 pp from 2005 to 2045, whereas in the two scenarios involving trade liberalization decreasing rates of 0.25 pp occur. PAO, however, encounters increasing TC rates (+0.5 pp) for the trade scenario (1) and constant rates for the other two scenarios. Finally, PAS is the only region where the trade scenario causes the lowest TC rates compared with the reference scenario and the other two policy scenarios. The sensitivity due to different population and GDP scenarios is lowest in the trade scenario, where only LAM and PAO show high variations and highest in the combined scenario, where all regions except AFR, CPA, and LAM face considerable variations.

[37] Another option for MAgPIE to increase total production, besides TC, is to expand cropland. Table 3 illustrates the change in total cropland over time and the total cropland in 2045 (in million hectares). In 2005, the difference of a livestock control policy becomes apparent. With lower livestock consumption cropland expansion is only half compared to the scenarios with business-as-usual consumption. However, in 2015 and 2025, the expansion increases further in the livestock scenario but decreases from 2035 on. Highest total expansion (+348 million hectare) is obtained in the reference scenario and lowest in the combined trade-livestock scenario (+156 million hectare). The sensitivity of those values against different GDP per

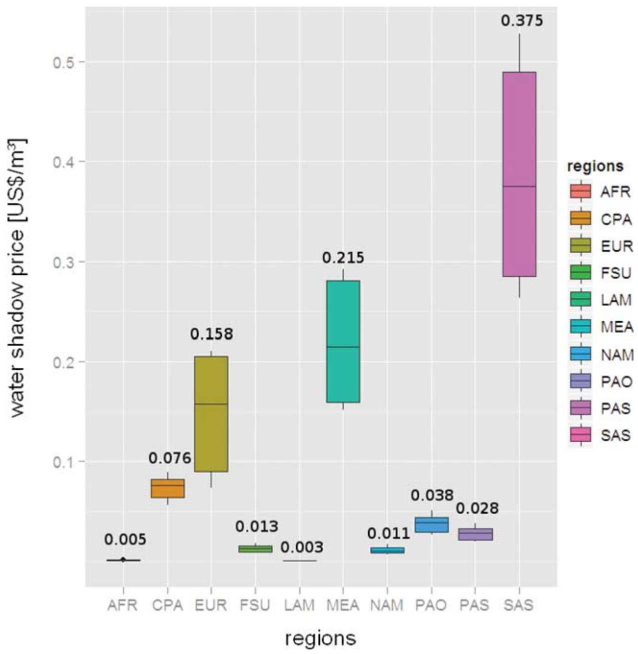

Figure 6. Sensitivity of the regional WSP (in US$/m) in 2045 for the trade, livestock and combined scenario under consideration of nine different population and GDP sensitivity scenarios. The boxplots display minimum, lower quartile, median, upper quartile, and maximum. Above the boxplots, the value of the default scenario is given.

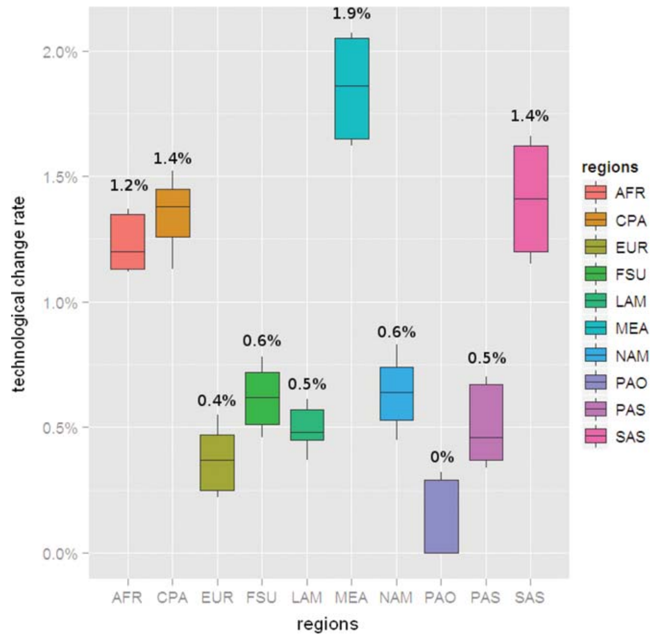

Figure 8. Sensitivity of the TC rates in 2045 under nine different population and GDP sensitivity scenarios. The boxplots display minimum, lower quartile, median, upper quartile, and maximum. Above the boxplots, the value of the default scenario is given.

capita scenarios is low. The highest value for total cropland in the reference scenario in 2045 is 1711 million hectare and the lowest is 1591 million hectare. The variations in the policy scenarios are slightly higher. For instance, in the combined scenario, the highest value is 1537 million hectare and the lowest is 1372 million hectare. In terms of area equipped for irrigation, we obtain an increase of 14% in the reference scenario until 2045, 11% in the trade scenario, 7% in the livestock scenario, and only 1% in the combined scenario.

4. Discussion

[38] The increasing pressure of agriculture on water availability has its origin in the extensive population growth and the resulting increase in food production during the last century [*Falkenmark et al.*, 1989; *Vörösmarty et al.*, 2000; *Kummu et al.*, 2010]. As we expect a further

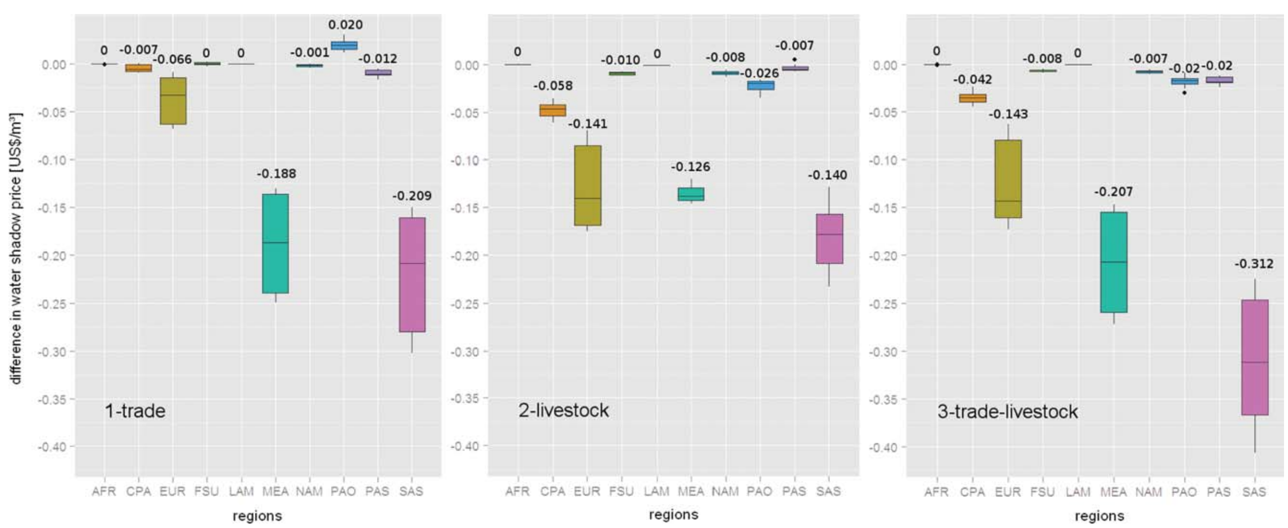

Figure 7. Sensitivity of the difference in regional WSP in 2045 under nine different population and GDP sensitivity scenarios. The boxplots display minimum, lower quartile, median, upper quartile, and maximum. Above the boxplots, the value of the default scenario is given.

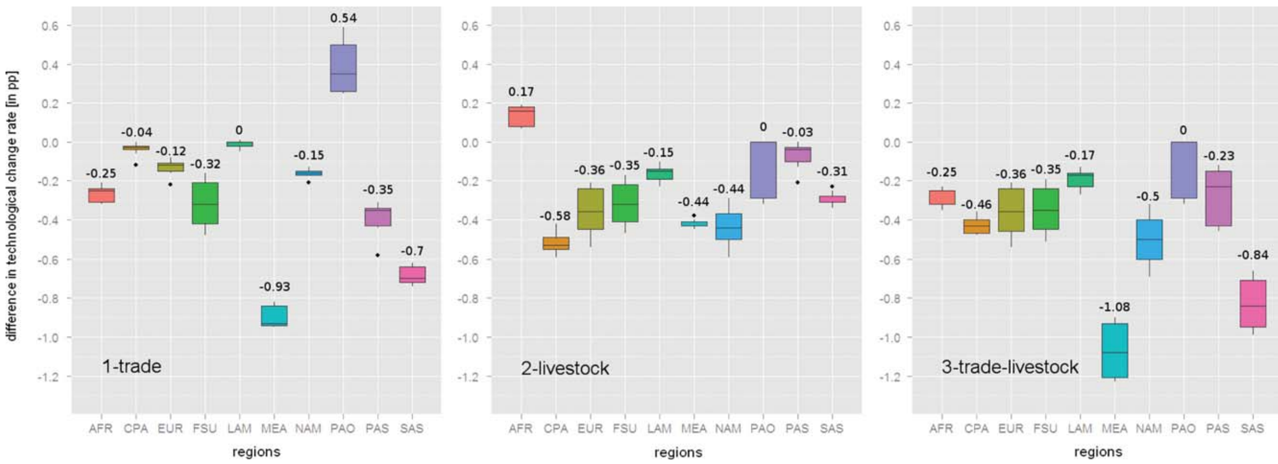

Figure 9. Sensitivity of the difference in TC rates in 2045 under nine different population and GDP sensitivity scenarios. The boxplots display minimum, lower quartile, median, upper quartile, and maximum. Above the boxplots the value of the default scenario is given.

increase in population and an even more dramatic increase in agricultural demand, the pressure on water resources will rise considerably throughout the coming decades. In order to quantify this relationship, we have developed an agroeconomic water scarcity indicator, the WSP.

4.1. Water Shadow Price

[39] The WSP is the outcome of coupling a biophysical vegetation model and an economic land use model. It links spatially explicit water withdrawal and availability with economic processes in the land use and agricultural sector. Hence, the WSP considers explicitly economic processes of water demand in an optimization approach, which has been consistently neglected by previous indicators [*Sauer et al.*, 2010]. It takes important economic drivers, such as income, trade, production costs, and productivity growth, into account which are crucial for assessing water scarcity. In general, the WSP provides a more comprehensive picture of water scarcity than purely biophysically based indicators.

[40] Before calculating the WSP, the amount of available irrigation water in MAgPIE is derived from water discharge (from LPJmL) reduced by an irrigation efficiency parameter. In most studies, irrigation efficiency is a static input or it changes only due to exogenous scenarios [i.e., *Fischer et al.*, 2007]. An exception is the model created by *Sauer et al*. 2010, which is able to invest endogenously in an improved irrigation system based on population growth. In contrast to this approach, we have implemented irrigation efficiency as a dynamic input depending on the level of economic development (GDP per capita). Although income does not explain the whole variation, we demonstrate with the regression analysis that it is strongly correlated to efficiency improvement (also confirmed by *Sauer et al*. [2010] and *Calzadilla et al*. [2011a]). Our irrigation efficiencies increase between 2% and 12% points from 2005 to 2045. *Fischer et al*. [2007] assume exogenous increases in efficiency of 10% per decade, whereas *Sauer et al*. [2010] are in line with our rather moderate estimates.

Table 3. Total Cropland Expansion (in Million Hectare) From 2005 Until 2045 and Total Cropland (in Million Hectare) in 2045

	Expansion					Total Cropland
Scenario	2005	2015	2025	2035	2045	2045
0-refernce	104	74	60	59	51	1648
1-trade	103	37	49	51	39	1580
2-livestock	53	69	60	36	7	1526
3-trade-livestock	53	41	40	11	10	1456

[41] The projected WSP of MAgPIE ranges between 0 and 0.3 US$/m^3 for 2005 and between 0 and 2 US$/m^3 for 2045. Comparing these values with real market prices of water led to biases since market prices are often highly determined by local policies (subsidies), market distortions (environmental externalities), or missing information. For instance, real prices in Europe vary between 0.01 US$/m^3 in Bulgaria and 1.4 US$/m^3 in Netherlands [*Berbel et al*., 2007]. Studies about WSPs are rare. One study assessed WSPs for Spain for 2005 and found a shadow price in average of 0.19–0.39 US$/m^3 [*Novo et al*., 2009], which fits well to our results for 2005.

4.2. Limitations of the Indicator

[42] The WSP has certain limitations to serve as an agroeconomic water scarcity indicator. First of all, it is based on blue water, ignoring the interactions and influences of green water on the agricultural system. Those are especially important in the livestock sector, where the differences of green and blue water use are huge [*Hoekstra and Chapagain*, 2007], comparing, for instance, extensive beef production on grasslands (mainly green water) with industrial livestock farming (partially fed with imported irrigated feed crops). Hence, more detailed water-related studies with a focus on the future development of livestock systems are needed. Further limitations are related to the MAgPIE model, since the shadow price itself is directly linked to the overall goal function of minimizing production costs. Important shortcomings of the model are missing direct production distortions like tariffs and subsidies as well as the consideration of only intraregional but no

interregional transport costs. Although those limitations reduce the WSP, others increase it. One is the demand representation in MAgPIE, which is exogenously given by regressions between income and calorie consumption (described in Appendix B). The exogenous implementation implies that price elasticities of demand are zero, i.e., consumption cannot be adjusted endogenously to changing prices. As a consequence, the model has less flexibility to substitute the demand, which results in higher shadow prices. Another limitation is irrigation efficiency. While it is a dynamic input dependent on economic development, it cannot be changed endogenously by investments. This may lower efficiency levels in the future, although the study by *Sauer et al*. [2010] reveals rather low levels/low rates of investment-related efficiency improvements.

4.3. Scenario Assessment and Uncertainty

[43] The most general finding of our scenario analysis is that water scarcity in all regions increases until 2050. In Sub-Saharan Africa and Latin America, it increases with low rates, whereas in South Asia and the Middle East/north Africa region with high rates. Although no other study has examined an agroeconomic water scarcity at high spatial resolution, we can at least compare our results with studies displaying regional values. *Rosegrant et al*. [2002] project water scarcity levels with the IMPACT-WATER model up to 2025 and show generally moderate increases with decreasing rates in developed countries. As in our study, they found strong increases in north Africa, Middle East, China, and India. In contrast to our findings, they also project high increases in Latin America.

[44] Our simulations indicate that with trade liberalization, the reallocation of agricultural land use can help to reduce regional water scarcity in the long run. This holds especially in world regions where water will become extremely scarce over the coming decades. The only exceptions to this rule are Australia, Japan, and parts of Central Asia (mainly Kazakhstan), where water becomes a bit scarcer. Other trade studies, like the CGE analysis by *Berrittella et al*. [2008], found rather small effects (changes in water use below 10%). In contrast to our results, trade liberalization leads to higher water use in the United States and China and lower water use in Japan, whereas the remaining regions encounter similar trends. Since the study highlights only the period 1997–2010, comparability is limited. The same model, GTAP-W, is used by *Calzadilla et al*. [2011b] for analyzing trade liberalization scenarios until 2050. Compared to our model, Australia has the highest increase in water scarcity due to liberalization, whereas Southeast Asia, South Asia, Middle East, and Former Soviet Union benefit from lower pressure on water resources. Simulations by the WATERSIM model confirm that increased trade between water-abundant regions and water-scarce regions avoid further stress on water scarcity [*de Fraiture et al*., 2007]. The comparison with our simulations has to be interpreted with caution since they assume perfect free trade, which is a more extreme scenario than ours.

[45] Agricultural trade is largely driven by economic forces. Local water prices, indicating the level of water scarcity, lead to more economic appreciation of water as a scarce resource and to more water-efficient trade from abundant to scarce regions. An improved system of agricultural trade also addresses the issue of local production risks as those will likely increase in the future due to climate change. Production failure in certain regions due to extreme weather events could be balanced out through trade from other production regions [*Fraser and Rimas*, 2010]. Examples for national policies are the reduction of export and import barriers for agricultural products, or on international level, the WTO negotiations, where the consequences of further trade liberalization and protection are discussed. Besides, chances for beneficial trade liberalization, which relax pressure on regional water scarcity, should not be overestimated in the short to medium term. As experiences from the WTO Doha Round show, political processes on the global level are slow and dominated by national interests instead of efficient resource use from global perspectives. Furthermore, developing countries would have to finance imports by foreign exchange [*Seckler et al*., 2000], which have to be generated by the export of other products. In the past, many countries in Africa and South Asia have not been successful in developing competitive products.

[46] The second policy option is a shift from a business-as-usual diet to a healthy livestock diet, which contains the same share of animal-based products for every world region. If this shift is simulated, the pressure on water scarcity in all regions is reduced, as plant-based calories contain less water in its production than animal-based calories. This is an unexpected outcome since the livestock share in some regions, for instance, in SAS and MEA, increases in the healthy livestock diet scenario. The reason behind the lower WSP is the linkage between regions through trade. Trade translates less animal-based consumption in the developed countries into lower pressure in water-scarce regions like India or the Middle East. As a consequence, the effects on WSP in developing regions are highest in the combined scenario of trade liberalization and diet shift, whereas in developed countries, the diet shift effects largely outweigh the trade effects. Possible policies to reduce consumption of animal products include the introduction of a tax on animal based products, a qualified ban on consumption or awareness raising and knowledge transfer through educational programs [*Deckers*, 2010]. An example for this is Denmark, which has recently introduced a tax on saturated fat to achieve a lower consumption of livestock products [*Smed*, 2012].

[47] To our knowledge, there is no other study that has quantified the effects of lower animal-based consumption in spatial detail. Yet, *Gerten et al*. [2011] found out that the likelihood for a country to be water scarce would be reduced, particularly in African countries, if animal calories were halved. *Renault and Wallender* [2000] analyzed the percentage of additional water, which is saved according to different scenarios until 2025. The scenario that replaces 50% of meat by vegetal products counts water savings of 23% and the one that replaces 50% of animal products yields in 39% savings. Comparing this to our healthy livestock diet scenario (scenario 2) without any trade changes, we calculated savings of 40% until 2025 and 28% until 2050. *Liu and Savenije* [2008] found positive effects of lower meat consumption for China and concluded that virtual water trade and improvement of rainfed agriculture are the more promising strategies. Other studies, examining livestock reducing scenarios, found positive effects on the reduction of greenhouse

gas emissions [*Popp et al*., 2010; *Stehfest et al*., 2009]) and the pressure on cropland [*Wirsenius et al*., 2010].

[48] The MAgPIE model has the unique feature of generating TC rates endogenously based on investments in agricultural research and development. Our analysis reveals a lower pressure on agricultural productivity due to the aforementioned policies. The average global annual rate of TC in agriculture until 2045 is 0.9% in the reference scenario, compared to 0.6% in the trade scenario, 0.7% in the healthy livestock diet scenario, and 0.5% in the combined scenario. At the regional level, those effects are much higher in regions like MEA and SAS but also NAM. We can state that increased trade and a healthy livestock diet not only help to reduce water scarcity but also to lower the pressure for intensification in agriculture. Furthermore, the policy scenarios lead to lower cropland expansion globally. As shown in *Schmitz et al*. [2012], this differs on a regional level, and trade liberalization leads to further deforestation in tropical regions like South America, with negative implications for greenhouse gas emissions. Area equipped for irrigation expands by 14% until 2045, which is roughly in line with the study by *Sauer et al*. [2010], who estimate an increase of 14% of the irrigated area until 2030. In this context, we have to emphasize again that no impacts of climate change are considered in this study. Those impacts are mainly changing temperature and precipitation patterns and have heterogeneous effects on the regional water balance. Especially in many developing regions, this implies further threats on water availability [*Gerten et al*., 2011; *Rockström et al*., 2009; *Vörösmarty et al*., 2000]. A detailed study by *Fischer et al*. [2007] concluded that climate change causes globally up to 20% more irrigation until 2080, which is of similar magnitude than the expansion required due to socioeconomic drivers in this time span.

[49] Our sensitivity analysis is focused on different population and GDP scenarios. Although we used extreme sensitivity scenarios, the variation in results is rather moderate. Water scarce regions like South Asia and the Middle East are most affected, but the ranking order is hardly affected by different demand projections. The study by *Schmitz et al*. [2012] estimates the sensitivity of MAgPIE regarding TC and land expansion and finds changing results in the range of −10% and +16% in terms of emissions and production costs. However, since only a limited number of model parameters have been tested, a more comprehensive sensitivity analysis would be necessary to reveal the whole range of possibilities.

[50] Overall, our analysis indicates that only one of the considered policy measures in this study is not enough to keep water scarcity at levels observed in 2005. Only the combination of both policies can reduce global WSPs in 2045 in most regions below the values in 2005. This does not hold for China, Australia, Japan, and countries in Sub-Saharan Africa, where additional strategies have to be developed in order to keep the pressure on water resources at current levels. Examples, which could be picked up by subsequent studies, are options to increase irrigation efficiency, improvements in infrastructure, institutional reforms, and also the issue of water pricing.

5. Conclusion and Policy Implications

[51] In many regions of the world, water is a scarce resource. Due to insufficient price signals, this is not yet recognized in all its consequences by many social factors. Many developing countries, which are heavily dependent on the agricultural sector and located in dry areas, are especially affected by water shortage. Water shortage is likely to lead to higher food prices threatening regional food security further.

[52] Under different GDP and population scenarios, the MAgPIE model computes food demand and generates spatially explicit projections of WSPs and regional TC rates. As water scarcity is increasing and severe in regions like South Asia, Middle East, and north Africa, trade liberalization and policies to control livestock consumption are promising measures to curtail water scarcity. The pressure to intensify is particularly reduced in importing regions, which are the regions with higher water scarcity. In the case of further trade liberalization, we found that intensification is less effective in terms of reducing water scarcity for developed countries than for developing countries. This is particularly important since developed countries have hampered further liberalization efforts in the past.

[53] Lower animal-based consumption in developed countries, as a second policy option, does not only reduce the domestic pressure on water but also reduce water scarcity in developing countries. However, as *Ridoutt et al*. [2011] points out, production of livestock-based goods is very diverse in terms of water consumption. Rather than condemning the whole animal sector, a focus on low-water input systems should be an alternative policy strategy in developed countries.

[54] In order to reach a level of water consumption that does not increase water scarcity in developing regions in the future despite population growth, it is not sufficient to count on trade liberalization and reduced livestock consumption in developed countries. Measures to improve water-use efficiency, such as investment in breeding of water-saving plants, the promotion of water-saving production systems, or improved irrigation infrastructure, are needed. Furthermore, incentives for improved water management have to be institutionalized. In many regions, water is seriously undervalued and lacking defined property rights, especially in the agricultural sector.

Appendix A: Regions and Products in MAgPIE

[55] The regional disaggregation of MAgPIE is shown in Table A1.

[56] MAgPIE distinguishes 16 different cropping activities and 5 livestock activities (Table A2).

Table A1. World Regions in MAgPIE

Abbreviation	Regions
AFR	Sub-Sahara Africa
CPA	Centrally planned Asia (including China)
EUR	Europe (including Turkey)
FSU	Former Soviet Union
LAM	Latin America
MEA	Middle East and north Africa
NAM	North America
PAO	Pacific OECD (Australia, Japan, and New Zealand)
PAS	Pacific Asia
SAS	South Asia (including India)

Table A2. Cropping and Livestock Activities in MAgPIE

Cropping Activities		Livestock Activities
Temperate cereals	Oil palm	Ruminant meat
Maize	Pulses	Pig meat
Tropical cereals	Potato	Poultry meat
Rice	Cassava	Eggs
Soybean	Sugar beet	Milk
Rapeseed	Sugarcane	
Groundnut	Cotton	
Sunflower	Others	

Appendix B: Future Demand in MAgPIE and Sensitivity Scenarios

[57] In MAgPIE, demand for agricultural products is fixed for every region and every time step and cannot be influenced by the optimization process. Future trends in food demand are computed as a function of income (measured in terms of GDP) per capita based on a cross-country regression. The underlining GDP scenarios are calculated by following the methodology proposed by *Hawksworth* [2006], who model the output with a Cobb-Douglas production function based on investment data from *Heston et al*. [2011]. We combine the GDP output scenarios with the three different U.N. population scenarios to get, in total, nine different GDP per capita scenarios (Table B1), which result in nine different scenarios for food demand. The scenario with the label *E* is taken as the default scenario in our study, whereas the other eight scenarios are used for the sensitivity analysis.

[58] For the calculation of food demand, we use the relation between total calories C_T and income I_{MER} (measured in market exchange rate per capita). This relation is defined by a power function and estimated with a fixed effect model with time-dependent variables. Equation (B1) shows the estimated function

$$C_T = \exp\left(2.83 \times 10^{-3} + 2.13 \times 10^{-3}\mathrm{years}\right) \cdot I_{\mathrm{MER}}^{0.16+\left(-3.12\times10^{-5}\mathrm{years}\right)}. \quad \text{(B1)}$$

[59] The results in 1995 were calibrated to food demand by *FAO* [2010]. Figure B1 illustrates the total consumption (in GJ) for the 10 world regions in MAgPIE until 2045. In Figure B1, it is differentiated between the business-as-usual diet scenario and the healthy livestock diet scenario, where

Table B1. Composition of the Nine Population and GDP Sensitivity Scenarios

Label	U.N. Population	GDP Growth
A	Low	Slow
B	Low	Moderate
C	Low	Fast
D	Medium	Slow
E (default)	Medium	Moderate
F	Medium	Fast
G	High	Slow
H	High	Moderate
I	High	Fast

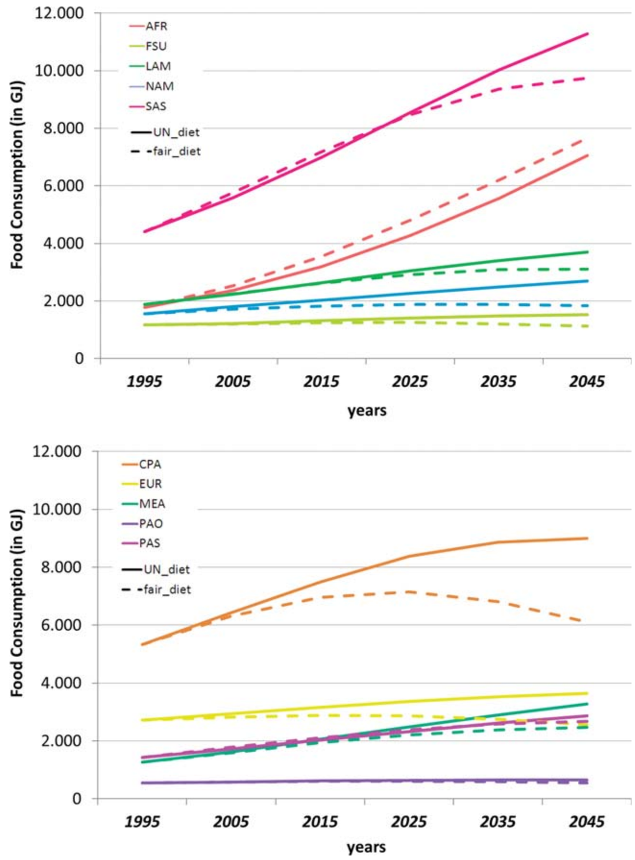

Figure B1. Food demand (in GJ) in the different world regions under the U.N. scenario (solid line) and the healthy livestock diet scenario (dashed line).

livestock consumption converts to a maximum share of 20%. Highest total consumption is projected for SAS, CPA, and AFR. In CPA, the growth rate stagnates after 2025 and the difference to the healthy livestock diet scenario is largest compared to the other regions.

[60] The drivers for the share of livestock products in total caloric intake are income, population growth, and time. In order to calculate the animal calorie consumption, the share of animal based calories C_{AS} is estimated by equation (B2).

$$C_{\mathrm{AS}} = \exp(-36.73 + 4.5 \cdot \ln(I_{\mathrm{MER}}) + 0.016 \cdot \mathrm{year} - 0.0021 \cdot \ln(I_{\mathrm{MER}}) \cdot \mathrm{year}) . \quad \text{(B2)}$$

[61] The results in 1995 were corrected by a constant share of fish products and calibrated to the livestock share by *FAO* [2010]. Figure B2 displays the resulting livestock consumption as a share of total consumption. The livestock-consumption share in CPA increases most, whereas the share decreases in regions, such as EUR or NAM. Applying the healthy livestock diet scenario, all regions move continuously to around 19%, the exception is PAO, where the share of fish products is comparatively large and the rate is reduced to around 14%. The share of fish is held

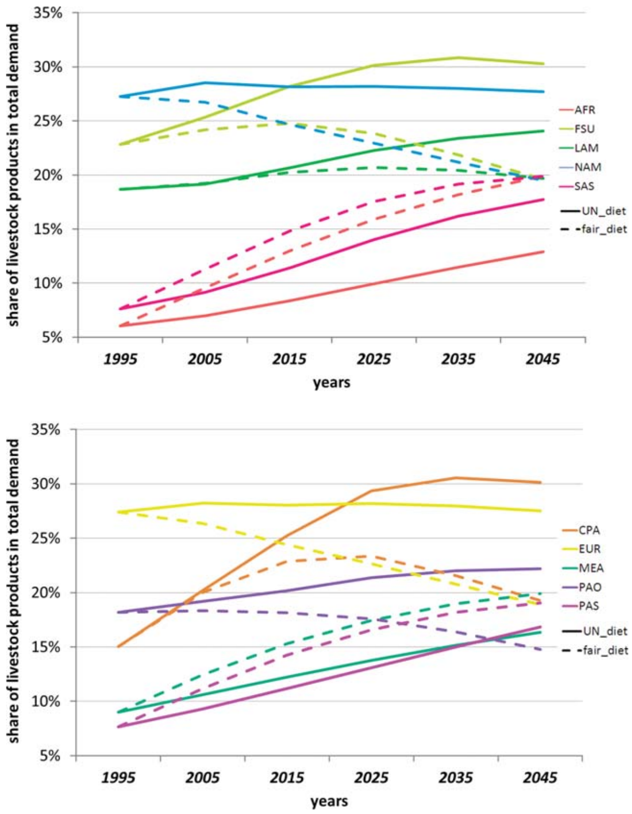

Figure B2. Livestock share of total demand in the different world regions under the U.N. scenario (solid line) and the healthy livestock diet scenario (dashed line).

constant over time since, in the current version of MAgPIE, we are not able to capture the dynamics of future fish demand in the model. Although this is a simplified assumption, the effect on the results is expected to be small as fish account only for 0%–2% of total calories and 4%–8% of animal calories across the regions [*FAO*, 2012].

Appendix C: Trade Implementation in MAgPIE

[62] The global food balance

$$\sum_i \frac{f^{\text{prod}}_{t,i,k}(x_t)}{1+p^{\text{seed}}_{i,k}} \geq \sum_i f^{\text{dem}}_{t,i,k}(x_t), \tag{C1}$$

with x as the variable for production, i as region, t as time, and k as production activity, shows the aggregated regional supply f^{prod}, which has to be equal or bigger than the aggregated regional demand f^{dem}. The supply is adjusted by the seed share p^{seed}, which accounts for the seeds used for the next farming season.

[63] Subsequently, we introduced excess demand and supply equations.

$$p^{xd}_{t,k} = \sum_i f^{\text{dem}}_{t,i,k}(x_t)\cdot\left(1-p^{sf}_{i,k}\right) : p^{sf}_{i,k} < 1. \tag{C2}$$

[64] The quantity of global excess demand p^{xd} for each production activity k is calculated by subtracting domestic demand (f^{dem}) from domestic production for the importing countries (for self-sufficiency ratio p^{sf} ¡ 1). Multiplying domestic demand with the self-sufficiency ratio ($f^{\text{dem}} \cdot p^{\text{sf}}$) results in domestic production.

$$p^{\text{xs}}_{t,i,k} = p^{\text{xd}}_{t,k}\cdot p^{\text{exshr}}_{t,i,k}. \tag{C3}$$

[65] The export shares p^{exshr} determine the amount of excess demand that is produced by the exporting regions.

[66] The trade balance equation

$$\frac{f^{\text{prod}}_{t,i,k}(x_t)}{1+p^{\text{seed}}_{i,k}} \geq p^{\text{tb}} \begin{cases} f^{\text{dem}}_{t,i,k}(x_t)+p^{\text{xs}}_{t,i,k} & : p^{\text{sf}}_{i,k} \geq 1 \\ f^{\text{dem}}_{t,i,k}(x_t)p^{\text{sf}}_{i,k} & : p^{\text{sf}}_{i,k} < 1 \end{cases} \tag{C4}$$

ensures the regional balance of supply and demand. For exporting regions, regional supply has to be at least equal to domestic demand plus the exported quantity. For importing regions, the regional supply has to be at least equal to domestic demand times the self-sufficiency. This holds true if the trade barrier reduction factor p^{tb} is equal to one. If p^{tb} is equal to zero, the equation becomes zero and everything is solved via the global trade balance (equation (B1)).

Appendix D: Irrigation Efficiencies in MAgPIE

[67] Figure D1 shows the irrigation efficiencies as result of the cross-country regression with income per capita. The values are based on population and income data of the default scenario *E*.

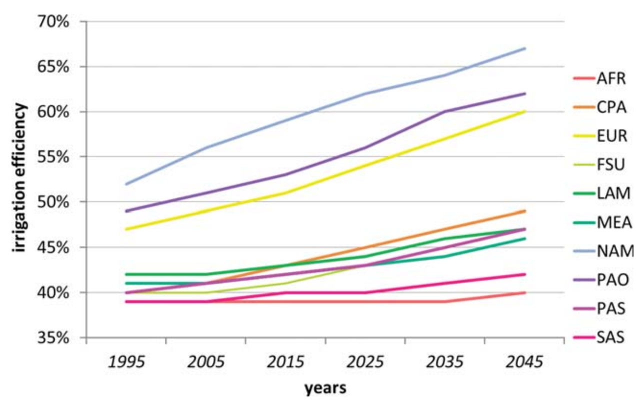

Figure D1. Irrigation efficiency in the 10 aggregated world regions from 1995 to 2045 based on the cross-country regression.

[68] **Acknowledgments.** We thank our colleagues at the land use research group of PIK for many fruitful discussions. We gratefully acknowledge the financial support by the German BMBF Projects "Hydrothermal Carbonization of Biomass," "NaWaMa Nachhaltiges Wassermanagement in einer globalisierten Welt," and "GLUES Global Assessment of Land Use Dynamics on Greenhouse Gas Emissions and Ecosystem Services." Furthermore, the research leading to these results has received funding from the European Union's Seventh Framework Programme (FP7/2007-2013) under grant agreement n°308329 (ADVANCE Project). Finally, we are grateful to three anonymous reviewers for their valuable comments, which substantially improved the paper.

References

Alcamo, J., P. Döll, T. Heinrichs, F. Kaspar, B. Lehner, T. Rösch, and S. Siebert (2003), Global estimates of water withdrawals and availability under current and future ''business-as-usual'' conditions, *Hydrol. Sci.*, *48*(3), 339–348.

Aucamp, D. C., and D. I. Steinberg (1982), The computation of shadow prices in linear programming, *J. Oper. Res. Soc.*, *33*(6), 557–565.

Berbel, J., A. Garrido, and J. Calatrava (2007), Water pricing and irrigation: A review of the European Experience, in *Irrigation Water Pricing—The Gap between Theory and Practice*, edited by F. Molle and J. Berkoff, pp. 295–327, CAB Int., Oxfordshire, U. K.

Berrittella, M., K. Rehdanz, R. S. J. Tol, and J. Zhang (2008), The impact of trade liberalization on water use: A computable general equilibrium analysis, *J. Econ. Integrat.*, *23*(3), 631–655.

Bondeau, A., P. Smith, S. Zaehle, S. Schaphoff, W. Cramer, D. Gerten, H. Lotze-Campen, C. Müller, M. Reichstein, and B. Smith (2007), Modelling the role of agriculture for the 20th century global terrestrial carbon balance, *Global Change Biol.*, *13*(3), 679–706.

Chavez, H. M. L., and S. Alipaz (2007), An integrated indicator based on basin hydrology, environment, life, and policy: The watershed sustainability index, *Water Resour. Manage.*, *21*, 883–895.

Cai, X., and M. W. Rosegrant (2002), Global water demand and supply projections—Part 1: A modeling approach, *Water Int.*, *27*(2), 159–169.

Calzadilla, A., K. Rehdanz, and R. S. J. Tol (2011a), Water scarcity and the impact of improved irrigation management: A computable general equilibrium analysis, *Agric. Econ.*, *42*(3), 305–323.

Calzadilla, A., K. Rehdanz, and R. S. J. Tol (2011b), Trade liberalization and climate change: A computable general equilibrium analysis of the impacts on global agriculture, *Water*, *3*, 526–550, doi:10.3390/w3020526.

Campbell, T. C., and T. Campbell (2006), *The China Study: Startling Implications for Diet, Weight Loss and Long-Term Health*, BenBella Books, Dallas, Tex.

Chapagain, A., and A. Hoekstra (2008), The global component of freshwater demand and supply: An assessment of virtual water flows between nations as a results of trade in agricultural and industrial products, *Water Int.*, *33*(1), 19–32.

Center for International Earth Science Information Network (CIESIN) (2000), *Gridded population of the world*, Center for Int. Earth Sci. Information Network (CIESIN) Columbia Univ., Int. Food Policy Res. Inst. (IFPRI) and World Resour. Inst. (WRI), Palisades, N. Y.

Conforti, P., and L. Salvatici (2004), Agricultural trade liberalisation in the Doha round—Alternative scenarios and strategic interactions between developed and developing countries, *FAO Commodity and Trade Policy Res. Working Pap. 10*, Rome, Italy.

Deckers, J. (2010), What policy should be adopted to curtail the negative global health impacts associated with the consumption of farmed animal products?, *Res. Publicat.*, *16*(1), 57–72.

de Fraiture, C. (2007), Integrated water and food analysis at the global and basin level. An application of WATERSIM, *Water Resour. Manage.*, *21*, pp. 185–198.

de Fraiture, C., D. Wichelns, J. Rockström, and E. Kemp-Benedict (2007), Looking ahead to 2050: Scenarios of alternative investment approaches, in *Water for Food, Water for Life: A Comprehensive Assesment of Water Management in Agriculture*, edited by D. Molden, pp. 91–145, Earthscan, London.

Delgado, C. L. (2003), Rising consumption of meat and milk in developing countries has created a new food revolution, *J. Nutr.*, *133*(11), 3907S–3910S.

Dietrich J.P., C. Schmitz, C. Müller, M. Fader, H. Lotze-Campen, A. Popp (2012), Measuring agricultural land-use intensity – A global analysis using a model-assisted approach, *Ecol. Modell., 232*, 109–118, doi: 10.1016/j.ecolmodel.2012.03.002.

Dietrich J.P., C. Schmitz, H. Lotze-Campen, A. Popp, C. Müller (2013), Forecasting technological change in agriculture – An endogenous implementation in a global land use model. *Technological Forecasting & Social Change*, doi: 10.1016/j.techfore.2013.02.003, in press.

Döll, P., and S. Siebert (2000), A digital global map of irrigated areas, *ICID J.*, *49*(2), 55–66.

Dollar, D., and A. Kraay (2004), Trade, growth and poverty, *Econ. J.*, *114*, 22–49.

Fader, M., S. Rost, C. Müller, A. Bondeau, and D. Gerten (2010), Virtual water content of temperate cereals and maize: Present and potential future patterns, *J. Hydrol.*, *384*(3–4), 218–231.

Fader, M., D. Gerten, M. Thammer, J. Heinke, H. Lotze-Campen, W. Lucht, and W. Cramer (2011), Internal and external green-blue agricultural water footprints of nations, and related water and land savings through trade, *Hydrol. Earth Syst. Sci.*, *15*, 1641–1660.

Falkenmark, M. (1989), The massive water scarcity threatening Africa—why isn't it being addressed, *Ambio*, *18*(2), 112–118.

Falkenmark, M., J. Lundqvist, and C. Widstrand (1989), Macro-scale water scarcity requires micro-scale approaches. Aspects of vulnerability in semi-arid development, *Natl. Resour. Forum 13*(4), 258–267.

Falkenmark M., A. Berntell, A.Jägerskog, J. Lundqvist, M. Matz, and H. Tropp (2007), *On the verge of a new water scarcity: A call for good governance and human ingenuity,* SIWI Policy Brief *11*, Stockholm Int. Water Inst. (SIWI).

Food and Agriculture Organization (FAO) (2010), FAOSTAT—Food and Agriculture Organization of the United Nations Statistics Division. [Available at http://faostat.fao.org/, accessed 11 July 2010.].

Food and Agriculture Organization (FAO) (2011), AQUASTAT—Database on investment costs in irrigation. [Available at http://www.fao.org/nr/water/aquastat/investment/index.stm/, accessed 23 July 2011.].

Food and Agriculture Organization (FAO) (2012), FAOSTAT—Food and Agriculture Organization of the United Nations Statistics Division. [Available at http://faostat.fao.org/, accessed 11 Dec. 2012.].

Fraser, E. D. G., and A. Rimas (2010), *Empires of Food: Feast, Famine, and the Rise and Fall of Civilizations*, Free Press, New York.

Fischer, G., F. N. Tubiello, H. van Velthuizen, and D. A. Wiberg (2007), Climate change impacts on irrigation water requirements: Effects of mitigation, 1990–2080, *Technol. Forecast. Social Change*, *74*(7), 1083–1107.

Gerten, D., S. Schaphoff, U. Haberlandt, W. Lucht, and S. Sitch (2004), Terrestrial vegetation and water balance: Hydrological evaluation of a dynamic global vegetation model, *J. Hydrol.*, *286*, 249–270.

Gerten, D., J. Heinke, H. Hoff, H. Biemans, M. Fader, and K. Waha (2011), Global water availability and requirements for future food production, *J. Hydrometeorol.*, *12*, 885–899, doi:10.1175/2011JHM1328.1.

Gleick, P. H., H. Cooley, and M. Morikawa (2009), *The Worlds Water 2008–2009: The Biennial Report on Freshwater Resources*, Island Press, Washington D.C., USA.

Godfray, H. C. J., J. R. Beddington, I. R. Crute, L. Haddad, D. Lawrence, J. F. Muir, J. Pretty, S. Robinson, S. M. Thomas, and C. Toulmin (2010), Food security: The challenge of feeding 9 billion people, *Science*, *327*(5967), 812–818.

Hanasaki, N., S. Kanae, T. Oki, K. Masuda, K. Motoya, N. Shirakawa, Y. Shen, and K. Tanaka (2008a), An integrated model for the assessment of global water—Part 1: Model description and input meteorological forcing, *Hydrol. Earth Syst. Sci.*, *12*(4), 1007–1025.

Hanasaki, N., S. Kanae, T. Oki, K. Masuda, K. Motoya, N. Shirakawa, Y. Shen, and K. Tanaka (2008b), An integrated model for the assessment of global water—Part 2: Applications and assessments, *Hydrol. Earth Syst. Sci.*, *12*(4), 1027–1037.

Hanasaki, N., T. Inuzuka, S. Kanae, and T. Oki (2010), An estimation of global virtual water flow and sources of water withdrawal for major crops and livestock products using a global hydrological model, *J. Hydrol.*, *384*(3-4), 232–244.

Hanjra, M. A., and M. E. Qureshi (2010), Global water crisis and future food security in an era of climate change, *Food Policy*, *35*(5), 365–377.

Hawksworth, J. (2006), The world in 2050: How big will the major emerging market economies get and how can the OECD compete, Price Waterhouse Coopers Report, London, UK.

Healy, S., R. Pearce, and M. Stockbridge (1998), The implications of the Uruguay round agreement on agriculture for developing countries. Training Material for Agricultural Planning, FAO (Food and Agriculture Organisation of the UN, Rome, Italy.

Heston A., R. Summers, and B. Aten (2011), Penn world table version 7.0, Center for Int. Comparisons of Production, Income and Prices at the University of Pennsylvania, Philadelphia, Pa.

Hoekstra, A. Y., and P. Q. Hung (2005), Globalisation of water resources: international virtual water flows in relation to crop trade, *Global Environ. Change*, *15*, 45–56.

Hoekstra, A. Y., and A. K. Chapagain (2007), Water footprints of nations: Water use by people as a function of their consumption pattern, *Water Resour. Manage.*, *21*(1), 35–48.

Islam, M. S., T. Oki, S. Kanae, N. Hanasaki, Y. Agata, and K. Yoshimura (2006), A grid-based assessment of global water scarcity including virtual water trading, *Water Resour. Manage.*, *21*, 19–33.

Konar, M., C. Dalin, S. Suweis, N. Hanasaki, A. Rinaldo, and I. Rodriguez (2011), Water for food: The global virtual water trade network, *Water Resour. Res.*, *47*, W05520, doi: 10.1029/2010WR010307.

Krause, M., H. Lotze-Campen, and A. Popp (2009), Spatially-explicit scenarios on global cropland expansion and available forest land in an integrated modelling framework, paper presented at the 27th International Association of Agricultural Economists Conference in Beijing, China, 16–22 Aug. 2009.

Kummu, M., P. J. Ward, H. de Moel, and O. Varis (2010), Is physical water scarcity a new phenomenon? Global assessment of water shortage over the last two millennia, *Environ. Res. Lett.*, *5*, 034006.

Liu, J., and H. H. G. Savenije (2008), Food consumption patterns and their effect on water requirement in China, *Hydrol. Earth Syst. Sci.*, *12*(3), 887–898.

Lotze-Campen, H., C. Müller, A. Bondeau, A. Jachner, A. Popp, and W. Lucht (2008), Food demand, productivity growth and the spatial distribution of land and water use: A global modeling approach, *Agric. Econ.*, *39*, 325–338.

Lutz, W., W. Sanderson, and S. Scherbov (2001), The end of population growth, *Nature*, *412*, 543–545.

Molden, D. (Ed.) (2007), *Water for Food, Water for Life: A Comprehensive Assessment of Water Management in Agriculture*, London: Earthscan.

Nakicenovic, N., and R. Swart (Eds.) (2000), *Special Report on Emisson Scenarios*, Cambridge Univ. Press, Cambridge, U. K.

Narayanan, B., and T. L. Walmsley (2008), *Global Trade, Assistance, and Production: The GTAP 7 Data Base*, Center for Global Trade Analysis, Purdue Univ.

Nelson, A. (2008), Estimated travel time to the nearest city of 50,000 or more people in year 2000, Global Environment Monitoring Unit—Joint Research Centre of the European Commission, Ispra, Italy. [Available at http://bioval.jrc.ec.europa.eu/products/gam/, accessed 30 July 2011.].

Novo, P., A. Garrido, and C. Varela-Ortega (2009), Are virtual water flows in Spanish grain trade consistent with relative water scarcity?, *Ecol. Econ.*, *68*(5), 1454–1564.

Ohlsson, L. (2000), Water conflicts and social resource scarcity, *Phys. Chem. Earth Part B*, *25*(3), 213–220.

Oki, T., and S. Kanae (2004), Virtual water trade and world water resources, *Water Sci. Technol.*, *49*(7), 203–209.

Oki, T., and S. Kanae (2006), Global hydrological cycles and world water resources, *Science*, *313*, 1068–1072.

Pingali, P. (2006), Westernization of Asian diets and the transformation of food systems: Implications for research and policy, *Food Policy*, *32*, 281–298.

Popp, A., H. Lotze-Campen, and B. Bodirsky (2010), Food consumption, diet shifts and associated non-CO_2 greenhouse gases from agricultural production, *Global Environ. Change 20*, 451–462.

Popp, A., J. P. Dietrich, H. Lotze-Campen, D. Klein, N. Bauer, M. Krause, T. Beringer, D. Gerten, and O. Edenhofer (2011), The economic potential of bioenergy for climate change mitigation with special attention given to implications for the land system, *Environ. Res. Lett.*, *6*(3), 034017.

Portmann, F., S. Siebert, and P. Döell (2010), MIRCA2000-Global monthly irrigated and rainfed crop areas around the year 2000: A new high-resolution data set for agricultural and hydrological modelling, *Global Biogeochem. Cycles 24*, GB1011, doi: 10.1029/2008GB003435.

Pimentel, D., and M. Pimentel (2003), Sustainability of meat-based and plant-based diets and the environment, *Am. J. Clin. Nutr.*, *78*(3), 660S–663S.

Ramsey, J. B. (1969), Tests for specification errors in classical linear least-squares regression analysis, *J. R. Stat. Soc. Ser. B*, *31*(2), 350–371.

Renault, D., and W. W. Wallender (2000), Nutritional water productivity and diets, *Agric. Water Manage.*, *45*(3), 275–296.

Ridoutt, B. G., P. Sanguansri, M. Freer, and G. S. Harper (2011), Water footprint of livestock: comparison of six geographically defined beef production systems, *Int. J. Life Cycle Assess.* (online first), 17:165–175, doi:10.1007/s11367-011-0346-y.

Rockström, J., M. Falkenmark, L. Karlberg, H. Hoff, S. Rost, and D. Gerten (2009), Future water availability for global food production: The potential of green water for increasing resilience to global change, *Water Resour. Res.*, *45*, W00A12, doi: 10.1029/2007WR006767.

Roeckner, E., et al. (2003), The atmospheric general circulation model ECHAM5. PART I: Model description, *Rep. 349*, Max Planck Inst. for Meteorol., Hamburg, Germany. [Available at http://www.mpimet.mpg.de.].

Rogers, D. H., F. R. Lamm, M. Alam, T. R. Trooien, G. A. Clark, P. L. Barnes, and K. Mankin (1997), *Efficiencies and Water Losses of Irrigation Systems, Irrig. Manage. Ser. MF-2243*, Kansas State Univ.

Rohwer, J., D. Gerten, and W. Lucht (2007), Development of functional types of irrigation for improved global crop modelling, PIK Rep. 104. Potsdam Institue for Climate Impact Research, Potsdam, Germany.

Rosegrant, M. W., and S. A. Cline (2003), Global food security: Challenges and policies, *Science*, *302*, 1917–1918.

Rosegrant, M. W., X. Cai, and S. A. Cline (2002), *World water and food to 2025: Dealing with scarcity, Food Policy Report*, International Food Policy Research Institute (IFPRI), Washington D.C., USA.

Rosegrant, M. W., C. Ringler, and T. Zhu (2009), Water for agriculture: maintaining food security under growing scarcity, *Annu. Rev. Environ. Resour.*, *34*, 205–222.

Rost, S., D. Gerten, A. Bondeau, W. Lucht, J. Rohwer, and S. Schaphoff (2008), Agricultural green and blue water consumption and its influence on the global water system, *Water Resour. Res.*, *44*, W09405, doi: 10.1029/2007WR006331.

Sauer, T., P. Havlik, U. A. Schneider, E. Schmid, G. Kindermann, and M. Obersteiner (2010), Agriculture and resource availability in a changing world: The role of irrigation, *Water Resour. Res.*, *46*, W06503, doi: 10.1029/2009WR007729.

Schmitz, C., J. P. Dietrich, H. Lotze-Campen, C. Müller, and A. Popp (2010), Implementing endogenous technological change in a global land-use model, paper presented at GTAP 13th Annual Conference in Penang, Malaysia, 9–11 June 2010.

Schmitz, C., A. Biewald, H. Lotze-Campen, A. Popp, J. P. Dietrich, B. Bodirsky, M. Krause, and I. Weindl (2012), Trading more food—Implications for land use, greenhouse gas emissions and the food system, *Global Environ. Change 22*(1), 189–209.

Seckler, D., D. Molden, U. Amarasinghe, and C. de Fraiture (2000), *Water Issues for 2025: A Research Perspective*, Int. Water Manage. Inst., Colombo.

Shiklomanov, I. A., and J. C. Rodda (Eds.) (2003), *World Water Resources at the Beginning of the Twenty-First Century*, Cambridge Univ. Press, New York.

Smakhtin, V., C. Revanga, and P. Döll (2004), A pilot global assessment of environmental water requirements and scarcity, *Water Int.*, *29*(3), 307–317.

Smed, S. (2012), Financial penalties on foods: The fat tax in Denmark, *Nutr. Bull.*, *37*(2), 142–147.

Sohngen, B., C. Tennity, and M. Hnytka (2009), Global forestry data for the economic modeling of land use, in *Economic Analysis of and Use in Global Climate Change Policy*, edited by T. W. Hertel, S. Rose, R. S. J. Tol, pp. 49–71, Routledge, New York.

Stehfest E., L. Bouwman, D. P. van Vuuren, M. G. J. den Elzen, B. Eickhout, and P. Kabat (2009), Climate benefits of changing diet, *Clim. Change*, *95*, 83–102.

United Nations (UN) (2011). *World Population Prospects: The 2010 Revision*, United Nations, Dep. of Economic and Social Affairs, Population Division, CD-ROM Edition, New York, N. Y.

Visser, H., and T. de Nijs (2006), The map comparison kit, *Environ. Modell. Software*, *21*(3), 346–358.

Vörösmarty, C. J., P. Green, J. Salisbury, and R. B. Lammers (2000), Global water resources: Vulnerability from climate change and population growth, *Science*, *289*(5477), 284–288.

Vörösmarty, C. J., et al. (2010), Global threats to human water security and river biodiversity, *Nature*, *467*, 555–561.

Weindl, I., H. Lotze-Campen, A. Popp, B. Bodirsky, and S. Rolinski (2010), Impacts of livestock feeding technologies on greenhouse gas emissions, paper presented at the IATRC Public Trade Policy Research and Analysis Symposium, Univ. Hohenheim, Stuttgart, Germany, 27–29 June 2010.

Wirsenius, S. (2000), *Human Use of Land and Organic Materials - Modeling the Turnover of Biomass in the Global Food System*, Chalmers Univ., Göteborg, Sweden.

Wirsenius, S., C. Azar, and G. Berndes (2010), How much land is needed for global food production under scenarios of dietary changes and livestock productivity increases in 2030?, *Agric. Syst.*, *103*(9), 621–638.

World Bank (2001), World development indicators 2001, World Bank Report No. 22099, The World Bank, Washington D. C., USA.